Phytochemistry 179 (2020) 112478

Contents lists available at ScienceDirect

Phytochemistry

journal homepage: www.elsevier.com/locate/phytochem

Synthesis of bilocularin A carbamate derivatives and their evaluation as leucine transport inhibitors in prostate cancer cells

Cohan Huxley [a], Mario Wibowo [a], Kah Yean Lum [a], Shelly Gordon [a], Sebastian D'Hyon [a], Hanyu Guan [a], Xueyi Wang [a], Yuxi Chen [a], Mingran Si [a], Mengchao Wang [a], Jonathan M. White [b], Kanu Wahi [c], Qian Wang [c], Jeff Holst [c], Rohan A. Davis [a,*]

[a] Griffith Institute for Drug Discovery, School of Environment and Science, Griffith University, Brisbane, QLD 4111, Australia
[b] School of Chemistry and Bio 21 Institute, The University of Melbourne, Parkville, VIC, 3010, Australia
[c] Translational Cancer Metabolism Laboratory, School of Medical Sciences and Prince of Wales Clinical School, The University of New South Wales, Sydney, NSW, 2052, Australia

ARTICLE INFO

Keywords:
Maytenus bilocularis
Celastraceae
Dihydro-β-agarofuran
Sesquiterpenoid
Bilocularin A
Semi-synthesis
Carbamate
Leucine transport inhibition
Prostate cancer
LNCaP

ABSTRACT

Large-scale extraction of the leaves of the Australian rainforest tree *Maytenus bilocularis* followed by extensive purification studies afforded the targeted and abundant dihydro-β-agarofuran, bilocularin A, in sufficient quantities (>500 mg) for detailed semi-synthetic chemistry. Eight bilocularin A carbamate analogues were synthesised using a series of commercially available isocyanate reagents in high purity (>95%) and variable yields (9–91%). All previously undescribed analogues were spectroscopically characterised using NMR, UV, IR and MS data. One compound afforded crystalline material and subsequent single crystal X-ray analysis (Cu-Kα) confirmed the chemical structure along with the absolute configuration. All compounds were evaluated for anti-proliferative activity against the human prostate cancer cell line LNCaP; none of the compounds showed significant (>50%) growth inhibition at 20 μM. Compounds were also tested for their ability to inhibit leucine transport in LNCaP cells, and two analogues showed moderate activity with IC_{50} values of 8.9 and 8.5 μM. This is the first reported synthesis of dihydro-β-agarofuran carbamate derivatives.

1. Introduction

The Celastraceae plant family is found throughout subtropical and tropical regions of the world, and has been shown to be a prolific source of bioactive natural products, the majority of which belong to the terpenoid structure class (Gao et al., 2007; Spivey et al., 2002). Mono-, sesqui-, di- and tri-terpenes are typically the most common natural constituents identified during chemical investigations on this family. One particular sub-class of terpenoids, the poly-oxygenated tricyclic sesquiterpenoids, also known as dihydro-β-agarofurans, has attracted the most interest from biologists and chemists alike over the past two decades (Gao et al., 2007; Spivey et al., 2002). Dihydro-β-agarofurans have been shown to exhibit a wide range of biological properties that include anti-inflammation (Zhou et al., 2019), anti-tumour (Perestelo et al., 2016), multidrug resistance reversal (Callies et al., 2015), neuroprotection (Fu et al., 2019), α-glucosidase inhibition (Sasikumar et al., 2018), and anti-fungal effects (Zhao et al., 2018).

For the past five years, the Davis research group has been actively researching the chemistry and biology of Australian Celastraceae species, including *Maytenus bilocularis* (F. Muell.) Loes (Wibowo et al., 2016a, 2018), *Denhamia pittosporoides* F. Muell. (Wibowo et al., 2016b), *Denhamia celastroides* (F. Muell.) Jessup (Levrier et al., 2015; Gordon et al., 2019; Wibowo et al., 2019), and *Celastrus subspicata* Hook. (Wibowo et al., 2017). This has resulted in the discovery of dihydro-β-agarofurans as leucine uptake inhibitors in the human prostate cancer cell line LNCaP, which were more potent than the L-type amino acid transporter (LAT) inhibitor, 2-aminobicyclo-(2,2,1)-heptane-2-carboxylic acid (BCH). We have also reported the most potent inhibitor of LAT (bilocularin G, $IC_{50} = 2.5$ μM) to date, which was isolated from the roots of *M. bilocularis* (Wibowo et al., 2018). These discoveries led us to further explore the potential of dihydro-β-agarofurans as LAT inhibitors by designing a semi-synthetic library based on this unique chemotype (Barnes et al., 2012; Choomuenwai et al., 2012; Davis et al., 2007; Egbewande et al., 2019, 2018; 2017; Kumar et al., 2015).

* Corresponding author.
E-mail address: r.davis@griffith.edu.au (R.A. Davis).

https://doi.org/10.1016/j.phytochem.2020.112478
Received 28 March 2020; Received in revised form 8 July 2020; Accepted 27 July 2020
Available online 14 August 2020
0031-9422/

Owing to bilocularin A (**1**) possessing multiple stereogenic centres (n=8), which confers a unique 3D shape to this molecule that has the potential to improve binding to biological targets (Feher and Schmidt, 2003; Gierasch et al., 2003; Grabowski et al., 2008), and this compound's high natural abundance (0.969% dry wt) from a sustainable source i.e. the leaves of the endemic rainforest tree *M. bilocularis* – a plant we are currently cultivating – we decided to undertake medicinal chemistry studies on this scaffold with the goal of making new small molecules that may ultimately impact drug discovery or chemical biology research. Herein we report the large-scale extraction and isolation of the known dihydro-*β*-agarofuran sesquiterpenoid, bilocularin A, from the leaves of *M. bilocularis* followed by the use of this tricyclic chiral scaffold in the solution-phase parallel synthesis of an eight-membered carbamate library (**2**–**9**) (Fig. 1). The evaluation of the semi-synthetic library for anti-proliferative effects and leucine uptake inhibition towards the prostate cancer cell LNCaP is also described.

2. Results and discussion

Large-scale CH_2Cl_2 extraction of the air-dried and ground leaves of *M. bilocularis* was undertaken followed by silica gel flash column chromatography (*n*-hexane–EtOAc gradient) to yield the targeted and previously reported dihydro-*β*-agarofuran, bilocularin A (**1**) in sufficient quantities (>500 mg) to enable the planned medicinal chemistry studies. Comparison of spectroscopic and spectrometric data for the re-isolated agarofuran **1** with literature values readily identified this compound as bilocularin A (Wibowo et al., 2016a).

While we had previously made several ester derivatives of bilocularin A, taking advantage of the secondary hydroxyl group at C-8 (Wibowo et al., 2016a), in these studies we hoped to generate derivatives incorporating the carbamate functionality, an important medicinal chemistry moiety often used in drug discovery or chemical biology applications (Gierasch et al., 2003). Following a modified literature procedure (Delebecq et al., 2013; Leenders et al., 1996; Schwetlick and Noack, 1995), we reacted scaffold **1** with eight commercially available (Sigma-Aldrich) isocyanates to generate a small library of bilocularin A carbamates in high purity (>95%) and low to high yield (9–91%). The chemical structures and NMR chemical shift assignments of all previously undescribed carbamate analogues (**2**–**9**) were determined following 1D (^{1}H, ^{13}C), 2D NMR (COSY, HSQC, HMBC and ROESY) and HRESIMS data analysis. UV, IR and $[\alpha]_D$ were also recorded for all previously undescribed analogues. An example of the reaction conditions and the structure elucidation and NMR assignment for compound **2** is detailed below.

A solution of bilocularin A (20 mg, 0.038 mmol) in anhydrous pyridine under a nitrogen atmosphere at 4 °C was treated with the commercial reagent phenylisocyanate (0.75 mmol, 20 mol excess) and stirred for 16 h. The reaction products were purified using semi-preparative C_{18} HPLC (MeOH/H_2O/0.1% TFA) followed by phenyl HPLC (MeOH/H_2O/0.1% TFA) to yield product **2** (17.2 mg) in respectable yield (70%) and high-purity (>95%).

The successful synthesis of compound **2** was initially confirmed by the (+)-LRESIMS data, which showed pseudomolecular ions at *m/z* 652 $[M+H]^+$ and 674 $[M+Na]^+$. Subsequent (+)-HRESIMS data indicated that **2** corresponded to a molecular formula of $C_{35}H_{41}NO_{11}$. The ^{1}H NMR spectrum of **2** in $CDCl_3$ showed signals for 16 methine protons, three methylene protons, and six methyl protons, whilst the ^{13}C NMR spectrum displayed a total of 31 unique carbon signals. Furthermore, COSY and key HMBC correlations enabled four spin systems and the positioning of the ester/carbamate moieties to be determined for analogue **2**, respectively (Fig. 2). For example the carbamate was definitely attached to C-8 based on a strong 3-bond HMBC correlation from H-8 [δ_H 5.55, dd (5.7, 4.3)] to the carbamate carbonyl at δ_C 152.8. Thus, based on this NMR and MS data, the planar structure of compound **2** was assigned as 8-phenylcarbamoyl bilocularin A. The relative and absolute configurations of **2**–**9** were all shown to be identical to that of the starting material, bilocularin A (**1**), based on ^{1}H–^{1}H coupling constants, ^{1}H NMR chemical shifts, ROESY data and specific rotation comparisons. Furthermore, a single-crystal X-ray diffraction experiment using Cu-K*α* radiation (Flack, 1983) was performed on compound **7** (Fig. 3), which unambiguously established the structure and absolute configuration of

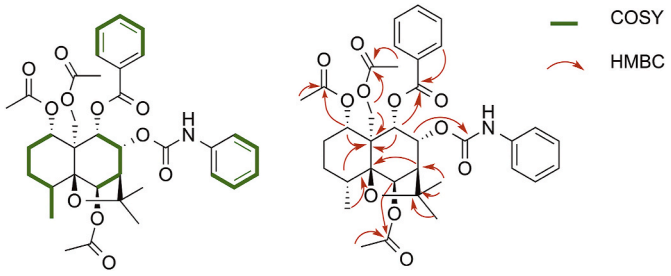

Fig. 2. COSY (in green) and key HMBC (in red) correlations of compound **2**. (For interpretation of the references to colour in this figure legend, the reader is referred to the Web version of this article.)

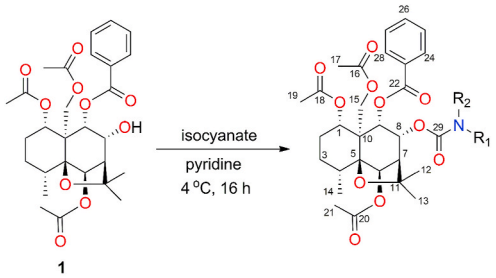

	2	3	4	5	6	7	8	9
R_1=	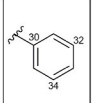	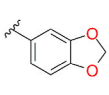		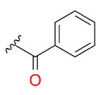	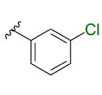	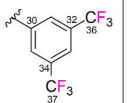	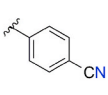	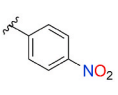
R_2=	H	H	H	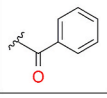	H	H	H	H

Fig. 1. Derivatisation reaction conditions for bilocularin A (**1**) and the resulting semi-synthetic carbamate library (**2**–**9**).

this particular bilocularin A derivative as 1*S*,4*R*,5*S*,6*R*,7*R*,8*R*,9*S*,10*S*. It is worth mentioning that the reaction of **1** with benzoyl isocyanate not only yielded compound **4**, but also the dibenzoylcarbamate derivative **5**.

Owing to our continuing interest in the discovery and development of natural products from Australian biota, which display activity against prostate cancer, compounds **1**–**9** were initially evaluated to determine their effects on cell viability (MTT, tetrazolium reduction assay) using the LNCaP human prostate cancer cell line (lymph node metastasis, androgen-sensitive). None of the compounds showed greater than 17% inhibition of cell viability on LNCaP cells at 20 μM after 72 h (Fig. 4a). In order to further investigate the biological activity of dihydro-β-agarofurans on cancer cells, compounds **1**–**9** were tested for their inhibitory effect on leucine uptake in prostate cancer cells. At 20 μM, compounds **4** and **5** showed significant inhibition of leucine uptake, reducing uptake by 31.3% and 22.5% of control, respectively (Fig. 4b). To determine the IC_{50} values, inhibitory curves were plotted using different doses of compounds **4** and **5** for the leucine uptake assay (Fig. 4c). The IC_{50} value for compound **4** was 8.9 μM and for compound **5** was 8.5 μM, with maximal inhibition around 50% of control uptake at 100 μM. Notably, the IC_{50} values for compounds **4** and **5** were lower than that of the parent compound, bilocularin A (**1**, IC_{50} = 124.5 μM) (Wibowo et al., 2016a). These data indicated that benzoyl carbamate substitution at C-8 improved leucine uptake inhibition for this particular series of dihydro-β-agarofurans. Moreover, these data further support the use of isolated natural products as scaffolds for the semi-synthesis of screening libraries (Barnes et al., 2016), which can lead to improvements in biological potency.

3. Conclusions

In conclusion, eight previously undescribed bilocularin A carbamate derivatives were synthesised by reacting the isolated natural product, bilocularin A (**1**), with a series of commercially available isocyanates. All semi-synthetic products were fully characterised by NMR, UV, IR, $[\alpha]_D$ and MS data. While no effect on cell viability over 3 days was observed for compounds **1**–**9** against the human prostate cancer cell line LNCaP at the tested concentration, analogues **4** and **5** showed moderate ability to inhibit leucine uptake in LNCaP cells. These studies highlight the potential of these novel compounds to be used as inhibitors of leucine uptake and should be investigated further. This is the first reported synthesis of dihydro-β-agarofuran carbamate derivatives at C-8. This unique agarofuran-based library has been added to the Davis open-access natural product-based library, which is housed and curated by Compounds Australia, Griffith University (www.compoundsaustralia.com), and is available for future collaborations in drug discovery and chemical biology research (Askin et al., 2018; Dilrukshi Herath et al., 2017; Zulfiqar et al., 2017).

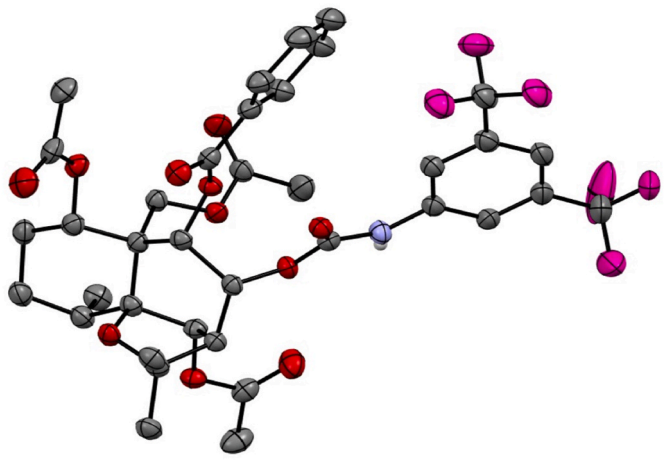

Fig. 3. ORTEP of bilocularin A carbamate analogue **7**; Hydrogen atoms, EtOH and H_2O molecules are omitted for clarity.

4. Experimental section

4.1. General experimental procedures

Melting points were measured using a Cole-Parmer melting point apparatus and were uncorrected. Optical rotations were determined on a JASCO P-1020 polarimeter. UV spectra were obtained using a JASCO V-650 UV/vis spectrophotometer. IR data were acquired using an attached Universal Attenuated Total Reflectance (UATR) Two module on a PerkinElmer spectrophotometer. NMR spectra were recorded on a Bruker AVANCE III HD 800 MHz NMR spectrometer at 25 °C. The ^1H and ^{13}C NMR chemical shifts were referenced to the solvent peaks for $CDCl_3$ at δ_H 7.26 and δ_C 77.16, respectively. LRESIMS data were recorded on a Waters ZQ ESI mass spectrometer or a Thermo Fisher MSQ Plus single quadrupole mass spectrometer. HRESIMS data were acquired on a 12 T SolariX XR FT-ICR-MS or Bruker maXis II ETD ESI-qTOF. X-ray diffraction data were collected on an Oxford-Diffraction Gemini S Ultra CCD diffractometer utilising CrysAlis software. Merck silica gel (40–63 μm, 230–400 mesh) packed into an open glass column (25 × 90 mm) was used for flash column chromatography. Thin layer chromatography (TLC) was carried out on Merck silica gel 60 F_{254} pre-coated aluminum plates and was observed using UV light at 254 and 365 nm. Alltech Davisil C_{18}-bonded silica (35–75 μm, 150 Å) was used for pre-adsorption work before HPLC separations, and the resulting material was packed into an Alltech stainless steel guard cartridge (10 × 30 mm). A Waters 600 pump fitted with a Waters 996 photodiode array detector and Gilson 717-plus autosampler was used for semi-preparative HPLC separations. A Thermo Betasil C_{18}-bonded silica column (5 μm, 120 Å, 150 × 21.2 mm), and a Thermo Betasil phenyl-bonded silica column (5 μm, 120 Å, 150 × 21.2 mm) were used for semi-preparative HPLC separations. A Fritsch Universal Cutting Mill Pulverisette 19 was used to grind the air-dried plant material. An Edwards Instrument Company Bio-line orbital shaker was used for plant extraction. All solvents used for chromatography, optical rotation, UV and MS were Honeywell Burdick & Jackson or Lab-Scan HPLC grade. H_2O was Millipore Milli-Q PF filtered. All chemical reagents were purchased from Sigma-Aldrich.

4.2. Plant material

Leaves of *Maytenus bilocularis* (F. Muell.) Loes (Celastraceae) were collected from Holland Park, Brisbane, Queensland, Australia during November of 2018. A voucher specimen (RAD076) has been deposited at the Griffith Institute for Drug Discovery, Griffith University, Brisbane, Australia.

4.3. Extraction and isolation

The air-dried and ground leaves of *M. bilocularis* (10 g) were extracted with CH_2Cl_2 (2 × 200 mL) at room temperature under constant shaking for 2 h. The organic solvent was filtered then evaporated under reduced pressure to give 1.44 g of CH_2Cl_2 extract that was pre-absorbed to silica gel (~10 g) before being chromatographed on a silica gel flash column (25 × 90 mm) using a 10% stepwise gradient solvent system of *n*-hexane–EtOAc (100% *n*-hexane to 50% EtOAc/50% *n*-hexane, 200 mL per elution step), the first two elution flushes (i.e. 100% *n*-hexane and 10% EtOAc/90% *n*-hexane) were discarded, then for the remaining flushes 20 fractions (i.e. 20 × 10 mL) were collected thus affording 80 fractions in total. Each fraction was analysed by TLC (*n*-hexane/EtOAc, 1:1) and those displaying the same TLC profile were combined to afford 10 fractions (F61–F70); all these fractions were analysed by ^1H NMR spectroscopy. Fractions 67–70 contained bilocularin A (**1**, 95.3 mg, 0.953% dry wt) in high-purity (>95%). This extraction and isolation protocol was repeated more than six times to

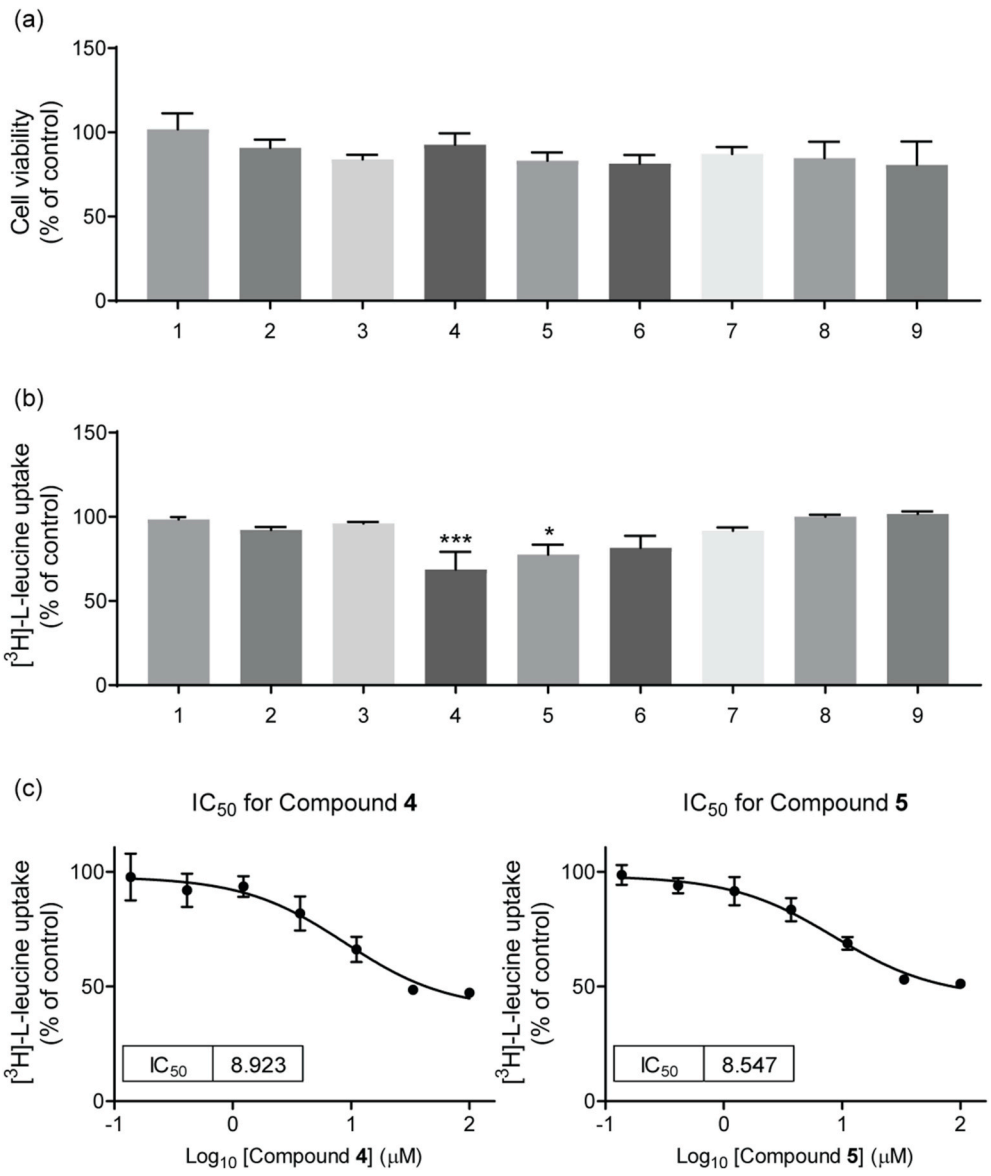

Fig. 4. Effects of compounds **1**–**9** on cell viability and leucine uptake in LNCaP cells (a) MTT cell growth assay was performed in LNCaP cells treated with compounds **1**–**9** at 20 μM for 72 h ($n = 3$, mean ± SEM) (b) [^{3}H]-L-leucine uptake was performed using 20 μM of compounds **1**–**9** in LNCaP cells ($n = 3$, mean ± SEM). Asterisks represent P-values: *P ⩽ 0.05; ***P ⩽ 0.001 for one-way analysis of variance by Dunnett's multiple comparison test (c) [^{3}H]-L-leucine uptake was performed at varying doses of compounds **4** and **5** to determine the IC_{50} values ($n = 3$, mean ± SEM).

yield >500 mg of the targeted scaffold, bilocularin A.

4.4. General preparation and purification of the carbamate derivatives **2**–**9**

A solution of bilocularin A (**1**, 20 mg, 0.038 mmol) in anhydrous pyridine (250 μL) under a nitrogen atmosphere at 4 °C was treated with a commercially available isocyanate (0.75 mmol, 20 mol excess) and stirred for 16 h. The reaction products were dried under nitrogen and pre-absorbed to C_{18}-bonded silica gel (~1 g) then packed into a guard cartridge, which was attached to the semi-preparative C_{18} HPLC column. HPLC separation conditions involved a linear gradient from 50% MeOH (0.1% TFA)–50% H_2O (0.1% TFA) to 95% MeOH (0.1% TFA)–5% H_2O (0.1% TFA) over 50 min, which was then held at 95% MeOH (0.1% TFA)–5% H_2O (0.1% TFA) for an additional 10 min, all at a flowrate of 9 mL/min. Sixty fractions (60 × 1 min) were collected from the start of the HPLC run. Fractions containing UV-active material from each separate HPLC run were analysed by ^{1}H NMR spectroscopy and LCMS, and relevant fractions with purity >95% were combined to afford the desired products. Compounds **2** and **7** were further purified using semi-preparative phenyl HPLC, in order to acquire the desired products in sufficient purity (>95%) for biological testing. The semi-pure samples (>70%) containing compounds **2** and **7** obtained from the C_{18} HPLC work were subjected to phenyl HPLC using identical solvent, time and flowrate conditions as those stated above for the C_{18} HPLC. This HPLC work afforded bilocularin A carbamate analogues **2** (17.2 mg, 70% yield), **3** (15.4 mg, 59% yield), **4** (12.3 mg, 48% yield), **5** (4.7 mg, 16% yield), **6** (15.5 mg, 60% yield), **7** (26.8 mg, 91% yield), **8** (14.0 mg, 45% yield), and **9** (2.3 mg, 9% yield).

4.5. Spectroscopic and spectrometric data

Compound **2**: stable white powder; $[\alpha]_D^{24}$–69 (*c* 0.1, MeOH); UV (MeOH) λ_{max} (log ε) 230 (5.11), 274 (3.92) nm; IR (UATR) ν_{max} 1737, 1313, 1225, 1068, 1051, 1022 cm^{-1}; ^{1}H NMR ($CDCl_3$, 800 MHz) δ_H 1.45 (3H, s, H-13), 1.49 (3H, s, H-19), 1.04 (3H, d, $J = 7.4$ Hz, H-14), 1.48 (1H, m, H-3α), 1.60 (3H, s, H-12), 1.71 (1H, m, H-2α), 1.78 (1H, m, H-2β), 2.13 (3H, s, H-21), 2.22 (1H, m, H-3β), 2.26 (1H, m, H-4), 2.29 (3H, br s, H-17), 2.54 (1H, br d, $J = 4.2$ Hz, H-7), 4.58 (1H, d, $J = 12.4$ Hz, H-15a), 5.08 (1H, br d, $J = 12.4$ Hz, H-15b), 5.40 (1H, dd, $J = 11.9$, 4.7 Hz, H-1), 5.55 (1H, dd $J = 5.7$, 4.2 Hz, H-8), 5.73 (1H, d, $J = 5.7$ Hz, H-9), 6.55 (1H, s, H-6), 6.97 (1H, br s, NH), 7.01 (1H, t, $J = 7.1$ Hz, H-33), 7.18

(2H, m, H-31, H-35), 7.20 (2H, m, H-32, H-34), 7.34 (2H, m, H-25, H-27), 7.48 (1H, m, H-26), 8.04 (2H, m, H-24, H-28); ^{13}C NMR ($CDCl_3$, 200 MHz) δ_C 15.5 (C-14), 20.9 (C-19), 21.5 (C-21), 21.7 (C-17), 23.1 (C-2), 24.6 (C-12), 26.5 (C-3), 30.6 (C-13), 33.5 (C-4), 51.0 (C-10), 53.4 (C-7), 60.7 (C-15), 71.8 (C-8), 73.4 (C-9), 74.7 (C-6), 79.5 (C-1), 81.4 (C-11), 90.8 (C-5), 118.9 (2C, C-31, C35), 123.7 (C-33), 128.6 (2C, C-25, C-27), 129.6 (C-23), 129.8 (2C, C-24, C-28), 129.1 (2C, C-32, C-34), 133.4 (C-26), 137.6 (C-30), 152.8 (C-29), 165.1 (C-22), 170.0* (C-18), 170.1* (C-20), 171.1 (C-16); (+)-LRESIMS *m/z* 652 $[M+H]^+$, 674 $[M+Na]^+$; (−)-LRESIMS *m/z* 650 $[M–H]^-$; (+)-HRESIMS *m/z* 652.2752 $[M+H]^+$ (calcd for $C_{35}H_{42}NO_{11}$, 652.2752), 674.2571 $[M+Na]^+$ (calcd for $C_{35}H_{41}NNaO_{11}$, 674.2572). *interchangeable signals.

Compound **3**: stable white powder; $[\alpha]_D^{24}$–25 (*c* 0.1, MeOH); UV (MeOH) λ_{max} (log ε) 232 (4.02), 294 (5.50) nm; IR (UATR) ν_{max} 1727, 1505, 1367, 1226, 1038 cm^{-1}; ^{1}H NMR ($CDCl_3$, 800 MHz) δ_H 1.03 (3H, d, J = 7.4 Hz, H-14), 1.44 (3H, s, H-13), 1.47 (1H, m, H-3α), 1.49 (3H, s, H-19), 1.59 (3H, s, H-12), 1.73 (1H, m, H-2α), 1.78 (1H, m, H-2β), 2.13 (3H, s, H-21), 2.22 (1H, m, H-3β), 2.25 (1H, m, H-4), 2.30 (3H, br s, H-17), 2.52 (1H, br s, H-7), 4.58 (1H, d, J = 13.1 Hz, H-15a), 5.08 (1H, br s, H-15b), 5.40 (1H, dd, J = 11.9, 4.7 Hz, H-1), 5.48 (1H, dd, J = 5.7, 4.3 Hz, H-8), 5.71 (1H, d, J = 5.7 Hz, H-9), 5.89 (2H, br s, H-36), 6.51 (1H, br s, H-6), 6.53 (1H, br d, J = 8.1 Hz, H-34), 6.63 (1H, d, J = 8.1 Hz, H-35), 6.79 (1H, br s, H-31), 6.93 (1H, br s, NH), 7.38 (2H, m, H-25, H-27), 7.51 (1H, m, H-26), 8.05 (2H, m, H-24, H-28); ^{13}C NMR ($CDCl_3$, 200 MHz) δ_C 15.5 (C-14), 20.9 (C-19), 21.5 (C-21), 21.7 (C-17), 23.1 (C-2), 24.5 (C-12), 26.5 (C-3), 30.6 (C-13), 33.5 (C-4), 51.0 (C-10), 53.3 (C-7), 60.8 (C-15), 71.7 (C-8), 73.4 (C-9), 74.7 (C-6), 79.5 (C-1), 81.4 (C-11), 90.8 (C-5), 101.3 (C-36), 102.1 (C-31), 108.1 (C-34), 112.3 (C-35), 128.7 (2C, C-25, C-27), 129.6 (C-23), 129.8 (2C, C-24, C-28), 131.8 (C-30), 133.4 (C-26), 144.1 (C-33), 148.0 (C-32), 153.2 (C-29), 165.1 (C-22), 170.1 (C-20), 170.2 (C-18), 171.1 (C-16); (+)-LRESIMS *m/z* 696 $[M+H]^+$, 718 $[M+Na]^+$; (−)-LRESIMS *m/z* 694 $[M–H]^-$; (−)-HRESIMS *m/z* 694.2473 $[M–H]^-$ (calcd for $C_{36}H_{40}NO_{13}$, 694.2505).

Compound **4**: stable white powder; $[\alpha]_D^{24}$–36 (*c* 0.1, MeOH); UV (MeOH) λ_{max} (log ε) 228 (4.27) nm; IR (UATR) ν_{max} 1735, 1369, 1230 cm^{-1}; ^{1}H NMR ($CDCl_3$, 800 MHz) δ_H 1.04 (3H, d, J = 7.4 Hz, H-14), 1.45 (3H, s, H-13), 1.46 (3H, s, H-19), 1.47 (1H, m, H-3α), 1.59 (3H, s, H-12), 1.72 (1H, m, H-2α), 1.77 (1H, m, H-2β), 2.12 (3H, s, H-21), 2.23 (3H, br s, H-17), 2.23 (1H, m, H-3β), 2.26 (1H, m, H-4), 2.57 (1H, br d, J = 4.3 Hz, H-7), 4.52 (1H, d, J = 13.2 Hz, H-15a), 5.27 (1H, d, J = 13.2 Hz, H-15b), 5.39 (1H, dd, J = 11.9, 4.7 Hz, H-1), 5.53 (1H, dd, J = 5.5, 4.3 Hz, H-8), 5.75 (1H, d, J = 5.5 Hz, H-9), 6.46 (1H, s, H-6), 7.41 (2H, dd, J = 7.9, 7.3 Hz, H-25, H-27), 7.45 (2H, dd, J = 7.9, 7.3 Hz, H-33, H-35), 7.53 (1H, t, J = 7.3 Hz, H-26), 7.57 (1H, t, J = 7.3 Hz, H-34), 7.84 (2H, d, J = 7.9 Hz, H-32, H-36), 8.13 (2H, d, J = 7.9 Hz, H-24, H-28), 8.60 (1H, s, NH); ^{13}C NMR ($CDCl_3$, 200 MHz) δ_C 15.4 (C-14), 20.9 (C-19), 21.4 (C-21), 21.8 (C-17), 23.0 (C-2), 24.5 (C-12), 26.5 (C-3), 30.6 (C-13), 33.5 (C-4), 50.9 (C-10), 53.0 (C-7), 60.5 (C-15), 73.1 (C-8), 73.2 (C-9), 74.4 (C-6), 79.7 (C-1), 81.5 (C-11), 90.8 (C-5), 127.9 (2C, C-32, C-36), 128.8 (2C, C-25, C-27), 128.9 (2C, C-33, C-35), 129.4 (C-23), 129.9 (2C, C-24, C-28), 132.8 (C-31), 133.1 (C-34), 133.7 (C-26), 150.4 (C-29), 164.9 (C-22), 165.2 (C-30), 169.9 (C-20), 170.0 (C-18), 171.6 (C-16); (−)-LRESIMS *m/z* 678 $[M–H]^-$; (+)-LRESIMS *m/z* 680 $[M+H]^+$; (−)-HRESIMS *m/z* 678.2532 $[M–H]^-$ (calcd for $C_{36}H_{40}NO_{12}$, 678.2556).

Compound **5**: stable white powder; $[\alpha]_D^{24}$–33 (*c* 0.1, MeOH); UV (MeOH) λ_{max} (log ε) 233 (4.09) nm; IR (UATR) ν_{max} 1734, 1230, 1101 cm^{-1}; ^{1}H NMR ($CDCl_3$, 800 MHz) δ_H 0.92 (3H, d, J = 7.4 Hz, H-14), 1.35 (3H, s, H-13), 1.40 (3H, s, H-19), 1.43 (1H, m, H-3α), 1.51 (3H, s, H-12), 1.65 (1H, m, H-2α), 1.70 (1H, m, H-2β), 1.96 (3H, s, H-21), 2.01(1H, br d, J = 4.1 Hz, H-7), 2.15 (3H, s, H-17), 2.18 (1H, m, H-4), 2.17 (1H, m, H-3β), 4.55 (1H, d, J = 13.2 Hz, H-15a), 4.67 (1H, br d, J = 13.2 Hz, H-15b), 5.34 (1H, dd, J = 11.9, 4.4 Hz, H-1), 5.43 (1H, dd, J = 6.0, 4.1 Hz, H-8), 5.66 (1H, d, J = 6.0 Hz, H-9), 6.52 (1H, s, H-6), 7.34 (4H, dd, J = 7.9, 7.5 Hz, H-33, H-35, H-40, H-42), 7.48 (2H, dd, J = 7.9, 7.5 Hz, H-25, H-27), 7.52 (2H, t, J = 7.5 Hz, H-34, H-41), 7.60 (1H, t, J = 7.5 Hz, H-26), 7.80 (4H, d, J = 7.9 Hz, H-32, H-36, H-39, H-43), 8.11 (2H, d, J = 7.9 Hz, H-24, H-28); ^{13}C NMR ($CDCl_3$, 200 MHz) δ_C 15.1 (C-14), 20.8 (C-19), 21.1 (C-21), 21.4 (C-17), 23.1 (C-2), 24.6 (C-12), 26.4 (C-3), 30.5 (C-13), 33.3 (C-4), 50.9 (C-10), 52.7 (C-7), 60.5 (C-15), 72.9 (C-9), 74.1 (C-6), 75.6 (C-8), 79.3 (C-1), 81.1 (C-11), 91.0 (C-5), 128.6 (2C, C-25, C-27), 128.9 (4C, C-33, C-35, C-40, C-42), 129.5 (5C, C-23, C-32, C-36, C-39, C-43), 130.4 (2C, C-24, C-28), 133.0 (2C, C-31, C-38), 133.5 (C-26), 133.7 (2C, C-34, C-41), 154.0 (C-29), 165.5 (C-22), 169.4 (C-20), 170.1 (C-18), 170.4 (2C, C-30, C-37), 170.9 (C-16); (+)-LRESIMS *m/z* 784 $[M+H]^+$, 806 $[M+Na]^+$; (−)-LRESIMS *m/z* 678 $[M–C_7H_6O]^-$, 782 $[M–H]^-$; (−)-HRESIMS *m/z* 678.2507 $[M–C_7H_6O]^-$ (calcd for $C_{36}H_{40}NO_{12}$, 678.2516); (+)-HRESIMS *m/z* 784.2963 $[M+H]^+$ (calcd for $C_{43}H_{46}NO_{13}$, 784.2964) and 806.2782 $[M+Na]^+$ (calcd for $C_{43}H_{45}NNaO_{13}$, 806.2783).

Compound **6**: stable white powder; $[\alpha]_D^{24}$–4 (*c* 0.1, MeOH); UV (MeOH) λ_{max} (log ε) 230 (4.15) nm; IR (UATR) ν_{max} 1725, 1596, 1530, 1210, 1050 cm^{-1}; ^{1}H NMR ($CDCl_3$, 800 MHz) δ_H 1.04 (3H, d, J = 7.5 Hz, H-14), 1.44 (3H, s, H-13), 1.47 (1H, m, H-3α), 1.50 (3H, s, H-19), 1.59 (3H, s, H-12), 1.72 (1H, m, H-2α), 1.77 (1H, m, H-2β), 2.12 (3H, s, H-21), 2.22 (1H, m, H-3β), 2.25 (1H, m, H-4), 2.28 (3H, br s, H-17), 2.53 (1H, br d, J = 4.1 Hz, H-7), 4.59 (1H, d, J = 13.2 Hz, H-15a), 5.10 (1H, br d, J = 13.2 Hz, H-15b), 5.40 (1H, dd, J = 12.0, 4.8 Hz, H-1), 5.50 (1H, dd, J = 5.6, 4.1 Hz, H-8), 5.72 (1H, d, J = 5.6 Hz, H-9), 6.48 (1H, s, H-6), 6.97 (1H, ddd, J = 8.0, 2.1, 2.1 Hz, H-35), 7.03 (1H, ddd, J = 8.0, 2.1, 2.1 Hz, H-33), 7.11 (1H, dd, J = 8.0, 8.0 Hz, H-34), 7.23 (1H, dd, J = 2.1, 2.1 Hz, H-31), 7.34 (2H, dd, J = 7.9, 7.4 Hz, H-25, H-27), 7.49 (1H, tt, J = 7.4, 1.2 Hz, H-26), 8.03 (2H, dd, J = 7.9, 1.4 Hz, H-24, H-28); ^{13}C NMR ($CDCl_3$, 200 MHz) δ_C 15.5 (C-14), 20.9 (C-19), 21.5 (C-21), 21.8 (C-17), 23.1 (C-2), 24.5 (C-12), 26.5 (C-3), 30.6 (C-13), 33.5 (C-4), 51.0 (C-10), 53.3 (C-7), 60.8 (C-15), 72.0 (C-8), 73.4 (C-9), 74.7 (C-6), 79.5 (C-1), 81.4 (C-11), 90.8 (C-5), 116.8 (C-33), 118.9 (C-31), 123.7 (C-35), 128.7 (2C, C-25, C-27), 129.5 (C-23), 129.7 (2C, C-24, C-28), 130.0 (C-34), 133.5 (C-26), 134.8 (C-30), 138.9 (C-32), 152.6 (C-29), 165.1 (C-22), 170.1 (2C, C-18, C-20), 171.2 (C-16); (+)-LRESIMS *m/z* 685 [^{35}Cl: $M+H]^+$, 687 [^{37}Cl: $M+H]^+$; (−)-LRESIMS *m/z* 684 [^{35}Cl: $M–H]^-$, 686 [^{37}Cl: $M–H]^-$; (−)-HRESIMS *m/z* 684.2214 $[M–H]^-$ (calcd for $C_{35}H_{39}^{35}ClNO_{11}$, 684.2217).

Compound **7**: stable colourless crystals (EtOH); mp 183–185 °C; $[\alpha]_D^{25}$–4 (*c* 0.1, MeOH); UV (MeOH) λ_{max} (log ε) 231 (4.18), 282 (5.99) nm; IR (UATR) ν_{max} 1723, 1386, 1277, 1126 cm^{-1}; ^{1}H NMR ($CDCl_3$, 800 MHz) δ_H 1.06 (3H, d, J = 7.4 Hz, H-14), 1.45 (3H, s, H-13), 1.49 (3H, s, H-19), 1.49 (1H, m, H-3α), 1.60 (3H, s, H-12), 1.74 (1H, m, H-2α), 1.76 (1H, m, H-2β), 2.14 (3H, s, H-21), 2.21 (1H, m, H-3β), 2.27 (1H, m, H-4), 2.29 (3H, s, H-17), 2.53 (1H, br d, J = 4.1 Hz, H-7), 4.61 (1H, d, J = 13.3 Hz, H-15a), 5.17 (1H, br d, J = 13.3 Hz, H-15b), 5.40 (1H, dd, J = 11.4, 5.0 Hz, H-1), 5.54 (1H, dd, J = 5.7, 4.1 Hz, H-8), 5.72 (1H, d, J = 5.7 Hz, H-9), 6.41 (1H, s, H-6), 7.31 (2H, m, H-25, H-27), 7.46 (1H, tt, J = 7.4, 1.3 Hz, H-26), 7.47 (1H, br s, H-33), 7.65 (2H, br s, H-31, H-35), 7.77 (1H, br s, NH), 8.03 (2H, m, H-24, H-28); ^{13}C NMR ($CDCl_3$, 200 MHz) δ_C 15.6 (C-14), 20.9 (C-19), 21.4 (C-21), 21.8 (C-17), 23.1 (C-2), 24.5 (C-12), 26.6 (C-3), 30.6 (C-13), 33.6 (C-4), 51.0 (C-10), 53.1 (C-7), 60.8 (C-15), 72.5 (C-8), 73.5 (C-9), 74.6 (C-6), 79.4 (C-1), 81.5 (C-11), 90.8 (C-5), 116.9 (sept, $^3J_{C\text{-}F}$ = 3.6 Hz, C-33), 118.4 (2C, br s, C-31, C-35), 123.1 (2C, q, $^1J_{C\text{-}F}$ = 272.1 Hz, C-36, C-37), 128.6 (2C, C-25, C-27), 129.4 (C-23), 129.6 (2C, C-24, C-28), 132.4 (2C, q, $^2J_{C\text{-}F}$ = 33.2 Hz, C-32, C-34), 133.6 (C-26), 139.4 (C-30), 152.6 (C-29), 165.0 (C-22), 170.0 (C-18), 170.2 (C-20), 171.7 (C-16); (+)-LRESIMS *m/z* 788 $[M+H]^+$; (−)-LRESIMS *m/z* 786 $[M–H]^-$; (−)-HRESIMS *m/z* 786.2348 $[M–H]^-$ (calcd for $C_{37}H_{38}F_6NO_{11}$, 786.2355).

Compound **8**: stable white powder; $[\alpha]_D^{25}$–64 (*c* 0.1, MeOH); UV (MeOH) λ_{max} (log ε) 232 (4.01) nm; IR (UATR) ν_{max} 1734, 1588, 1533, 1368, 1229, 1095 cm^{-1}; ^{1}H NMR ($CDCl_3$, 800 MHz) δ_H 1.03 (3H, d, J = 7.5 Hz, H-14), 1.43 (3H, s, H-13), 1.47 (3H, s, H-19), 1.48 (1H, m, H-3α), 1.57 (3H, s, H-12), 1.72 (1H, m, H-2α), 1.75 (1H, m, H-2β), 2.12 (3H, s, H-21), 2.20 (1H, m, H-3β), 2.23 (3H, s, H-17), 2.26 (1H, m, H-4), 2.51

(1H, br d, $J = 4.2$ Hz, H-7), 4.62 (1H, d, $J = 13.1$ Hz, H-15a), 5.06 (1H, br d, $J = 13.1$ Hz, H-15b), 5.39 (1H, dd, $J = 11.4$, 5.2 Hz, H-1), 5.50 (1H, dd, $J = 5.7$, 4.2 Hz, H-8), 5.71 (1H, d, $J = 5.7$ Hz, H-9), 6.40 (1H, s, H-6), 7.28 (2H, m, H-31, H-35), 7.29 (2H, dd, $J = 8.2$, 7.4 Hz, H-25, H-27), 7.45 (2H, m, H-32, H-34), 7.48 (1H, tt, $J = 7.4$, 1.4 Hz, H-26), 7.88 (1H, br s, NH), 7.99 (2H, br dd, $J = 8.2$, 1.4 Hz, H-24, H-28); ^{13}C NMR ($CDCl_3$, 200 MHz) δ_C 15.5 (C-14), 20.8 (C-19), 21.4 (C-21), 21.7 (C-17), 23.1 (C-2), 24.5 (C-12), 26.5 (C-3), 30.6 (C-13), 33.5 (C-4), 51.0 (C-10), 53.1 (C-7), 60.8 (C-15), 72.2 (C-8), 73.4 (C-9), 74.6 (C-6), 79.3 (C-1), 81.3 (C-11), 90.7 (C-5), 106.2 (C-33), 118.4 (2C, C-31, C-35), 119.0 (C-36), 128.6 (2C, C-25, C-27), 129.4 (C-23), 129.6 (2C, C-24, C-28), 133.2 (2C, C-32, C-34), 133.4 (C-26), 142.1 (C-30), 152.3 (C-29), 164.9 (C-22), 170.0 (C-18), 170.2 (C-20), 171.3 (C-16); (+)-LRESIMS *m/z* 677 $[M+H]^+$; (−)-LRESIMS *m/z* 675 $[M-H]^-$; (−)-HRESIMS *m/z* 675.2562 $[M-H]^-$ (calcd for $C_{36}H_{39}N_2O_{11}$, 675.2559).

Compound **9**: stable white powder; $[\alpha]_D^{25}$–42 (*c* 0.1, MeOH); UV (MeOH) λ_{max} (log ε) 228 (4.83), 262 (3.87) nm; IR (UATR) ν_{max} 1724, 1507, 1211, 1050 cm^{-1}; ^{1}H NMR ($CDCl_3$, 800 MHz) δ_H 1.05 (3H, d, $J =$ 7.6 Hz, H-14), 1.45 (3H, s, H-13), 1.49 (3H, s, H-19), 1.50 (1H, m, H-3α), 1.60 (3H, s, H-12), 1.73 (1H, m, H-2α), 1.76 (1H, m, H-2β), 2.15 (3H, s, H-21), 2.23 (1H, m, H-3β), 2.26 (3H, s, H-17), 2.28 (1H, m, H-4), 2.52 (1H, br d, $J = 4.3$ Hz, H-7), 4.64 (1H, d, $J = 13.1$ Hz, H-15a), 5.10 (1H, br d, $J = 13.1$ Hz, H-15b), 5.40 (1H, dd, $J = 11.4$, 4.9 Hz, H-1), 5.53 (1H, dd, $J = 5.7$, 4.3 Hz, H-8), 5.73 (1H, d, $J = 5.7$ Hz, H-9), 6.40 (1H, s, H-6), 7.32 (2H, dd, $J = 7.8$, 7.5 Hz, H-25, H-27), 7.34 (2H, m, H-31, H-35), 7.48 (1H, tt, $J = 7.5$, 1.4 Hz, H-26), 8.01 (2H, m, H-24, H-28), 8.07 (2H, m, H-32, H-34); ^{13}C NMR ($CDCl_3$, 200 MHz) δ_C 15.6 (C-14), 20.9 (C-19), 21.5 (C-21), 21.8 (C-17), 23.2 (C-2), 24.5 (C-12), 26.6 (C-3), 30.6 (C-13), 33.6 (C-4), 51.1 (C-10), 53.2 (C-7), 61.0 (C-15), 72.4 (C-8), 73.5 (C-9), 74.7 (C-6), 79.3 (C-1), 81.5 (C-11), 90.8 (C-5), 118.0 (2C, C-31, C-35), 125.2 (2C, C-32, C-34), 128.7 (2C, C-25, C-27), 129.5 (C-23), 129.7 (2C, C-24, C-28), 133.5 (C-26), 143.1 (C-33), 144.0 (C-30), 152.3 (C-29), 165.0 (C-22), 170.1 (C-18), 170.3 (C-20), 171.5 (C-16); (+)-LRESIMS *m/z* 697 $[M+H]^+$, 719 $[M+Na]^+$; (−)-LRESIMS *m/z* 695 $[M-H]^-$; (+)-HRESIMS *m/z* 719.2422 $[M+Na]^+$ (calcd for $C_{35}H_{40}N_2NaO_{13}$, 719.2423).

4.6. X-ray crystallography analysis

Intensity data for bilocularin carbamate analogue **7** were collected on a Rigaku Synergy Dual-source diffractometer using Cu-Kα radiation, the temperature during data collection was maintained at 100.0 (1) K using an Oxford Cryosystems cooling device. Colourless crystals of **7** were obtained by crystallisation from EtOH. The structure was solved by direct methods and difference Fourier Synthesis (Sheldrick, 2008) and refined by full matrix least squares refinement on F^2 using the WinGX (Farrugia, 1999) software package incorporating SHELXL-2013 (Sheldrick, 2015). Thermal ellipsoid plots were generated using the Mercury software (Macrae et al., 2008). Hydrogen atoms bound to the carbon atom were placed at their idealised positions using appropriate AFIX instructions in SHELXL, and included in subsequent refinement cycles. Hydrogen atoms attached to oxygen were located from difference Fourier maps and refined freely with isotropic displacement parameters. Full cif deposition resides with the Cambridge Crystallographic Data Centre (CCDC No. 1978780). Copies can be obtained free of charge on application at the following address: http://www.ccdc.cam.ac.uk/cgi-bin/catreq.cgi).

Crystal data for bilocularin carbamate analogue (**7**). $C_{37}H_{39}F_6NO_{11}.(CH_3CH_2OH).(H_2O)$ $M = 851.77$, orthorhombic, space group $P2_12_12_1$, $a = 15.2815$ (1), $b = 19.3373$ (1), $c = 28.2764$ (1) Å, $U = 8355.76$ (8) Å^3, $Z = 8$, Z' $= 2$ $D_c = 1.354$ g cm^{-3}, $\mu = 1.020$ mm^{-1}, Crystal size: 0.33 × 0.25 × 0.16 mm 320,357 reflections collected, 17,653 unique ($R_{int} = 0.106$), $R = 0.041$ [16,946 reflections with $I > 2\sigma(I)$], w$RF^2 = 0.111$ (all data). Absolute Structure Parameter −0.09 (3), GOF = 1.045.

4.7. Cell viability assay

LNCaP cells were obtained from the American Type Culture Collection (ATCC, Manassas, VA, USA) and were cultured in RPMI-1640 media (Thermo Fisher Scientific) supplemented with 10% FBS (Thermo Fisher Scientific) at 37 °C in an atmosphere containing 5% CO_2 and maintained in log phase growth. Cell viability as a function of metabolic activity was measured by the MTT assay [3–(4,5–dimethylthiazol–2–yl)–2,5–diphenyl tetrasodium bromide]. Briefly, LNCaP (7000 cells per well) were seeded for 24 h into 96-well tissue culture plates (Corning, NY, USA) and treated with 20 μM dose of the indicated compounds. Compounds were dissolved in DMSO and diluted in growth medium (final concentration 0.2%). Control cells were treated with the equivalent dose of DMSO (negative control). After 72 h, metabolic activity was measured by adding 10 μL of MTT solution (Millipore) and incubated at 37 °C for 4 h, prior to addition of 100 μL of isopropanol/HCl solution and mixed thoroughly. Plates were read at 570 nm and 630 nm in a Spectra MAX 900 plate reader. Results were plotted as percentages of the absorbance observed in control wells. Each data point was measured in triplicate and repeated in at least three independent experiments.

4.8. Leucine transport inhibition assay

The [^{3}H]-L-leucine uptake was performed as detailed previously (Wang et al., 2011). Briefly, LNCaP cells were cultured in RPMI media. After collecting and counting, cells (5×10^4/well) were incubated with 0.3 μCi [^{3}H]-L-leucine (200 nM; PerkinElmer) in leucine-free RPMI media (Invitrogen) with 10% (v/v) dialysed FBS in the presence of 20 μM of each compound for 30 min at 37 °C. Cells were collected, transferred to filter paper using a 96-well plate harvester (Tomtec Cell harvester), dried, exposed to scintillation fluid and counts measured using a liquid scintillation counter (PerkinElmer). One-way analysis of variance (GraphPad Prism) was used to identify the compounds that significantly inhibited leucine uptake when compared to the DMSO control. To determine IC_{50} values, different concentrations of identified inhibitors were used for the leucine uptake assay. Each data point was determined in triplicate and repeated in three independent experiments.

Declaration of competing interest

The authors declare that they have no known competing financial interests or personal relationships that could have appeared to influence the work reported in this paper.

Acknowledgements

The authors acknowledge the National Health and Medical Research Council (NHMRC) for financial support (Grant APP1024314 to R.A.D.) and thank the Australian Research Council (ARC) for support towards NMR and MS equipment (Grant LE140100119, LE0668477 and LE0237908) and financial support (Grant LP120200339 to R.A.D.). R.A.D. holds a New Concept Grant funded by It's a Bloke Thing through the Prostate Cancer Foundation of Australia's Research Program. This study was also supported by the Movember Revolutionary Team Award Targeting Advanced Prostate Cancer (Q.W. and J.H.) and the Australian Government Department of Health. K.Y.L. and M.W. thank Griffith University for Ph.D. scholarships (GUPRS and GUIPRS).

Appendix A. Supplementary data

Supplementary data to this article can be found online at https://doi.org/10.1016/j.phytochem.2020.112478.

References

Askin, S., Bond, T.E.H., Sorenson, A.E., Moreau, M.J.J., Antony, H., Davis, R.A., Schaeffer, P.M., 2018. Selective protein unfolding: a universal mechanism of action for the development of irreversible inhibitors. Chem. Commun. 54, 1738–1741. https://doi.org/10.1039/C8CC00090E.

Barnes, E.C., Choomuenwai, V., Andrews, K.T., Quinn, R.J., Davis, R.A., 2012. Design and synthesis of screening libraries based on the muurolane natural product scaffold. Org. Biomol. Chem. 10, 4015–4023. https://doi.org/10.1039/c2ob00029f.

Barnes, E.C., Kumar, R., Davis, R.A., 2016. The use of isolated natural products as scaffolds for the generation of chemically diverse screening libraries for drug discovery. Nat. Prod. Rep. 33, 372–381. https://doi.org/10.1039/C5NP00121H.

Callies, O., Sánchez-Cañete, M.P., Gamarro, F., Jiménez, I.A., Castanys, S., Bazzocchi, I. L., 2015. Restoration of chemosensitivity in P-glycoprotein-dependent multidrug-resistant cells by dihydro-β-agarofuran sesquiterpenes from *Celastrus vulcanicola*. J. Nat. Prod. 78, 736–745. https://doi.org/10.1021/np500903a.

Choomuenwai, V., Andrews, K.T., Davis, R.A., 2012. Synthesis and antimalarial evaluation of a screening library based on a tetrahydroanthraquinone natural product scaffold. Bioorg. Med. Chem. 20, 7167–7174. https://doi.org/10.1016/j.bmc.2012.09.052.

Davis, R.A., Pierens, G.K., Parsons, P.G., 2007. Synthesis and spectroscopic characterisation of a combinatorial library based on the fungal natural product 3-chloro-4-hydroxyphenylacetamide. Magn. Reson. Chem. 45, 442–445. https://doi.org/10.1002/mrc.1984.

Delebecq, E., Pascault, J.-P., Boutevin, B., Ganachaud, F., 2013. On the versatility of urethane/urea bonds: reversibility, blocked isocyanate, and non-isocyanate polyurethane. Chem. Rev. 113, 80–118. https://doi.org/10.1021/cr300195n.

Dilrukshi Herath, H.M.P., Preston, S., Hofmann, A., Davis, R.A., Koehler, A.V., Chang, B. C.H., Jabbar, A., Gasser, R.B., 2017. Screening of a small, well-curated natural product-based library identifies two rotenoids with potent nematocidal activity against *Haemonchus contortus*. Vet. Parasitol. 244, 172–175. https://doi.org/10.1016/j.vetpar.2017.07.005.

Egbewande, F.A., Coster, M.J., Jenkins, I.D., Davis, R.A., 2019. Reaction of papaverine with Baran diversinates^{TM}. Molecules 24, 3938. https://doi.org/10.3390/molecules24213938.

Egbewande, F.A., Nilsson, N., White, J.M., Coster, M.J., Davis, R.A., 2017. The design, synthesis, and anti-inflammatory evaluation of a drug-like library based on the natural product valerenic acid. Bioorg. Med. Chem. Lett 27, 3185–3189. https://doi.org/10.1016/j.bmcl.2017.05.021.

Egbewande, F.A., Sadowski, M.C., Levrier, C., Tousignant, K.D., White, J.M., Coster, M. J., Nelson, C.C., Davis, R.A., 2018. Identification of gibberellic acid derivatives that deregulate cholesterol metabolism in prostate cancer cells. J. Nat. Prod. 81, 838–845. https://doi.org/10.1021/acs.jnatprod.7b00929.

Farrugia, L.J., 1999. WinGX suite for small-molecule single-crystal crystallography. J. Appl. Crystallogr. 32, 837–838. https://doi.org/10.1107/S0021889899006020.

Feher, M., Schmidt, J.M., 2003. Property distributions: differences between drugs, natural products, and molecules from combinatorial chemistry. J. Chem. Inf. Comput. Sci. 43, 218–227. https://doi.org/10.1021/ci0200467.

Flack, H.D., 1983. On enantiomorph-polarity estimation. Acta Crystallogr. A 39, 876–881. https://doi.org/10.1107/S0108767383001762.

Fu, Y., Wang, W., Gong, Q., Zhang, H., Zhao, W., 2019. Neuroprotective dihydro-β-agarofuran-type sesquiterpenes from the seeds of *Euonymus maackii*. J. Nat. Prod. 82, 3096–3103. https://doi.org/10.1021/acs.jnatprod.9b00701.

Gao, J.-M., Wu, W.-J., Zhang, J.-W., Konishi, Y., 2007. The dihydro-β-agarofuran sesquiterpenoids. Nat. Prod. Rep. 24, 1153–1189. https://doi.org/10.1039/B601473A.

Gierasch, T.M., Shi, Z., Verdine, G.L., 2003. Extensively stereodiversified scaffolds for use in diversity-oriented library synthesis. Org. Lett. 5, 621–624. https://doi.org/10.1021/ol027116f.

Gordon, S., Wibowo, M., Wang, Q., Holst, J., Davis, R.A., 2019. Dihydro-β-agarofurans from the Australian rainforest plant *Denhamia celastroides* that inhibit leucine transport in prostate cancer cells. Magn. Reson. Chem. 57, 101–109. https://doi.org/10.1002/mrc.4801.

Grabowski, K., Baringhaus, K.-H., Schneider, G., 2008. Scaffold diversity of natural products: inspiration for combinatorial library design. Nat. Prod. Rep. 25, 892–904. https://doi.org/10.1039/B715668P.

Kumar, R., Sadowski, M.C., Levrier, C., Nelson, C.C., Jones, A.J., Holleran, J.P., Avery, V. M., Healy, P.C., Davis, R.A., 2015. Design and synthesis of a screening library using the natural product scaffold 3-chloro-4-hydroxyphenylacetic acid. J. Nat. Prod. 78, 914–918. https://doi.org/10.1021/np500856u.

Leenders, R.G.G., Ruytenbeek, R., Damen, E.W.P., Scheeren, H.W., 1996. Highly Diastereoselective Synthesis of Anomeric β-*O*-glycopyranosyl Carbamates from Isocyanates. Synthesis (Stuttg), pp. 1309–1312. https://doi.org/10.1055/s-1996-4377, 1996.

Levrier, C., Sadowski, M.C., Nelson, C.C., Healy, P.C., Davis, R.A., 2015. Denhaminols A–H, dihydro-β-agarofurans from the endemic Australian rainforest plant *Denhamia celastroides*. J. Nat. Prod. 78, 111–119. https://doi.org/10.1021/np500740f.

Macrae, C.F., Bruno, I.J., Chisholm, J.A., Edgington, P.R., McCabe, P., Pidcock, E., Rodriguez-Monge, L., Taylor, R., van de Streek, J., Wood, P.A., 2008. Mercury CSD 2.0 - new features for the visualization and investigation of crystal structures. J. Appl. Crystallogr. 41, 466–470. https://doi.org/10.1107/S0021889807067908.

Perestelo, N.R., Jiménez, I.A., Tokuda, H., Vázquez, J.T., Ichiishi, E., Bazzocchi, I.L., 2016. Absolute configuration of dihydro-β-agarofuran sesquiterpenes from *Maytenus jelskii* and their potential antitumor-promoting effects. J. Nat. Prod. 79, 2324–2331. https://doi.org/10.1021/acs.jnatprod.6b00469.

Sasikumar, P., Sharathna, P., Prabha, B., Varughese, S., Kumar, A.N., Sivan, V.V., Sherin, D.R., Suresh, E., Manojkumar, T.K., Radhakrishnan, K.V., 2018. Dihydro-β-agarofuran sesquiterpenoids from the seeds of *Celastrus paniculatus* Willd. and their α-glucosidase inhibitory activity. Phytochem. Lett. 26, 1–8. https://doi.org/10.1016/j.phytol.2018.04.011.

Schwetlick, K., Noack, R., 1995. Kinetics and catalysis of consecutive isocyanate reactions. Formation of carbamates, allophanates and isocyanurates. J. Chem. Soc. Perkin Trans. 2, 395–402. https://doi.org/10.1039/P29950000395.

Sheldrick, G.M., 2015. Crystal structure refinement with SHELXL. Acta Crystallogr. C 71, 3–8. https://doi.org/10.1107/S2053229614024218.

Sheldrick, G.M., 2008. A short history of SHELX. Acta Crystallogr. A 64, 112–122. https://doi.org/10.1107/S0108767307043930.

Spivey, A.C., Weston, M., Woodhead, S., 2002. Celastraceae sesquiterpenoids: biological activity and synthesis. Chem. Soc. Rev. 31, 43–59. https://doi.org/10.1039/b000678p.

Wang, Q., Bailey, C.G., Ng, C., Tiffen, J., Thoeng, A., Minhas, V., Lehman, M.L., Hendy, S. C., Buchanan, G., Nelson, C.C., Rasko, J.E.J., Holst, J., 2011. Androgenreceptor and nutrient signaling pathways coordinate the demand for increased amino acid transport during prostate cancer progression. Canc. Res. 71, 7525–7536. https://doi.org/10.1158/0008-5472.CAN-11-1821.

Wibowo, M., Forster, P.I., Guymer, G.P., Hofmann, A., Davis, R.A., 2019. Using UHPLC-MS profiling for the discovery of new dihydro-β-agarofurans from Australian Celastraceae plant extracts. Molecules 24, 859. https://doi.org/10.3390/molecules24050859.

Wibowo, M., Levrier, C., Sadowski, M.C., Nelson, C.C., Wang, Q., Holst, J., Healy, P.C., Hofmann, A., Davis, R.A., 2016a. Bioactive dihydro-β-agarofuran sesquiterpenoids from the Australian rainforest plant *Maytenus bilocularis*. J. Nat. Prod. 79, 1445–1453. https://doi.org/10.1021/acs.jnatprod.6b00190.

Wibowo, M., Wang, Q., Holst, J., White, J.M., Hofmann, A., Davis, R.A., 2018. Dihydro-β-agarofurans from the roots of the Australian endemic rainforest tree *Maytenus bilocularis* act as leucine transport inhibitors. Phytochemistry 148, 71–77. https://doi.org/10.1016/j.phytochem.2018.01.009.

Wibowo, M., Wang, Q., Holst, J., White, J.M., Hofmann, A., Davis, R.A., 2017. Celastrofurans A–G: dihydro-β-agarofurans from the Australian rainforest vine *Celastrus subspicata* and their inhibitory effect on leucine transport in prostate cancer cells. J. Nat. Prod. 80, 1918–1925. https://doi.org/10.1021/acs.jnatprod.7b00220.

Wibowo, M., Wang, Q., Holst, J., White, J.M., Hofmann, A., Davis, R.A., 2016b. Dihydro-β-agarofurans from the Australian endemic rainforest plant *Denhamia pittosporoides* inhibit leucine transport in prostate cancer cells. Asian J. Org. Chem. 5, 1461–1466. https://doi.org/10.1002/ajoc.201600462.

Zhao, X., Xu, S., Yin, M., Wang, X., Wang, Q., Shan, Y., Chen, Y., Liu, F., Guo, S., Feng, X., 2018. Six new dihydro-β-agarofuran sesquiterpenes from the stems and leaves of *Monimopetalum chinense* and their antimicrobial activities. Phytochem. Lett. 27, 160–166. https://doi.org/10.1016/j.phytol.2018.07.024.

Zhou, L., He, Q.-J., Lu, L.-W., Zhao, F., Zhang, Y., Huang, X.-X., Lin, B., Song, S.-J., 2019. Tripterfordins A–O, dihydro-β-agarofuran sesquiterpenoids from the leaves of *Tripterygium wilfordii*. J. Nat. Prod. 82, 2696–2706. https://doi.org/10.1021/acs.jnatprod.9b00089.

Zulfiqar, B., Jones, A.J., Sykes, M.L., Shelper, T.B., Davis, R.A., Avery, V.M., 2017. Screening a natural product-based library against kinetoplastid parasites. Molecules 22, 1715. https://doi.org/10.3390/molecules22101715.